

## Research Article

# Bifurcation Analysis and Quenching Chaos in Brushless DC Motor Based on Dither Signals

Shun-Chang Chang 

Department of Mechanical and Automation Engineering, Da-Yeh University, Changhua, 515006, Taiwan (R.O.C.)  
E-mail: changsc@mail.dyu.edu.tw

**Received:** 27 September 2024; **Revised:** 2 January 2025; **Accepted:** 12 February 2025

**Abstract:** This study investigates bifurcation and chaos dynamics in brushless direct current (DC) motor (BLDCM) through analyses of time response, Poincaré maps and frequency spectra. A chaos suppression approach is then proposed and detailed. To identify the initiation of chaotic motion in BLDCM, Lyapunov exponents and dimensions are utilized. Subsequently, the study implements the suggested method by introducing an external input, referred to as a dither signal, into the chaotic BLDCM system. The effectiveness of the proposed control method was determined by simulations.

**Keywords:** bifurcation, chaos, BLDCM, Lyapunov exponent, dither

**MSC:** 65L05, 34K06, 34K28

## 1. Introduction

Brushless DC motors (BLDCMs) have become widely across various fields, including electric vehicles [1, 2], aerospace [3], motion control systems [4], etc. These motors excel due to their higher power density, enhanced efficiency, and extended lifespan compared to traditional brushed counterparts [5, 6]. The nonlinear characteristics of such systems often give rise to phenomena like bifurcation and chaos [7, 8]. Effectively controlling or predicting their performance requires a thorough understanding of the impact of these nonlinearities. The stability and dynamics of nonlinear systems in BLDCM systems have been widely studied [9–11]. Research shows that under certain parameter conditions, motors may exhibit chaotic behavior, with erratic torque variations. This work aims to explore the nonlinear dynamics of BLDCMs and propose an effective strategy to mitigate chaos. A range of numerical methods, such as bifurcation diagrams, phase portraits, Poincaré maps, frequency spectra, and Lyapunov exponents, are employed to identify periodic and chaotic behaviors. Among these, Lyapunov exponents have proven to be the most reliable for assessing sensitivity to initial conditions [12]. In the current study, Lyapunov exponents are used to confirm the presence of chaotic behaviors in BLDCMs.

While some degree of chaotic behavior is manageable, it can significantly hinder performance and reduce the operational range of many electrical and mechanical devices. Controlling chaos in motors is particularly challenging due to the presence of numerous interdependent nonlinear variables. Recent advancements have introduced various control strategies for chaotic motion in BLDCMs [13–15], including nonlinear state feedback control [13], adaptive control [14],

and fuzzy control [15]. This study examines the selection of BLDCM parameters, along with external inputs or loads, under which chaotic behavior occurs. To enhance system performance or prevent chaos, it is often necessary to convert a chaotic behavior into a stable periodic motion. By introducing an external input, known as a dither signal, chaos can be effectively managed before nonlinearities become problematic. The use of dither signals for improving nonlinear system performance is well-documented, with the primary advantage being their simplicity, as they do not require any measurements for implementation. Dither signals have also been successfully applied in practical nonlinear systems [16–19]. For instance, Fuh and Tung [16] demonstrated the conversion of chaotic motion to a periodic orbit in circuit systems. However, Liaw and Tung [17] employed dither smoothing techniques to control a noisy chaotic system. Tung and Chen [18] developed a method for identifying a closed-loop DC motor system with unknown parameters and nonlinearities. Chang et al. [19] utilized dither signals to manage chaotic behaviors in permanent magnet synchronous motor for electric vehicles.

In this work, we focus on improving the performance of BLDCMs and mitigating chatter vibration by transforming chaotic motions into stable periodic orbits. The injection of a dither signal is proposed as a simple yet efficient approach to enhance nonlinear system performance. Simulation results confirm the effectiveness and practicality of the proposed method.

## 2. Analysis of chaos in BLDCMs

Following references [20–22], the governing equations of the BLDCM system are reformulated using an affine transformation and a single time-scale adjustment [23]. This process enables the derivation of a dimensionless mathematical representation, expressed as follows:

$$\frac{d\tilde{i}_q}{d\tilde{t}} = \tilde{u}_q - \tilde{i}_q - \tilde{\omega}\tilde{i}_d + \rho\tilde{\omega} \quad (1)$$

$$\frac{d\tilde{i}_d}{d\tilde{t}} = \tilde{u}_d - \delta\tilde{i}_d + \tilde{\omega}\tilde{i}_q \quad (2)$$

$$\frac{d\tilde{\omega}}{d\tilde{t}} = \sigma(\tilde{i}_q - \tilde{\omega}) + \eta\tilde{i}_q\tilde{i}_d - \tilde{T}_L \quad (3)$$

where  $\tilde{i}_q$  and  $\tilde{i}_d$  represent currents along the restructured direct and quadrature axes;  $\tilde{\omega}$  denotes the transformed angular speed of the motor;  $\tilde{u}_q$  and  $\tilde{u}_d$  indicate the voltages along the same axes;  $\tilde{T}_L$  corresponds the external load torque after transformation. Structural parameters  $\rho$ ,  $\delta$ ,  $\sigma$ , and  $\eta$  characterize the dynamics of the motor under these conditions. Setting  $y_1 = \tilde{i}_q$ ,  $y_2 = \tilde{i}_d$  and  $y_3 = \tilde{\omega}$ , Equations (1)-(3) are reformulated as follows:

$$\dot{y}_1 = \tilde{u}_q - y_1 - y_2y_3 + \rho y_3 \quad (4)$$

$$\dot{y}_2 = \tilde{u}_d - \delta y_2 + y_1y_3 \quad (5)$$

$$\dot{y}_3 = \sigma(y_1 - y_3) + \eta y_1y_2 - \tilde{T}_L \quad (6)$$

where the dot indicates derivation with respect to  $\tilde{t}$ . Table 1 lists the parameter values of the above equations [24].

**Table 1.** Parameters used in simplified BLDCM model [24]

Symbol	Parameter value
$\rho$	60
$\tilde{u}_q$	0.168
$\tilde{u}_d$	20.66
$\delta$	0.875
$\eta$	0.26
$\tilde{T}_L$	0.53

Numerical simulations were performed to explore the behaviors of the BLDCM system based on Equations (4)-(6). The ordinary differential equations were solved using the IMSL library's DIVPRK subroutine in FORTRAN [25]. Initial conditions ( $y_1(0) = 0.01, y_2(0) = 0.01, y_3(0) = 0.01$ ) and time step ( $1 \times 10^{-3}$ ) were applied. The results, shown in Figure 1, reveal that the system undergoes its first period-doubling bifurcation at  $\sigma = 4.08$ . Chaotic motion appeared in region II, while region III shows a period-3 motion, culminating in chaotic dynamics in region IV [26]. Further analysis, including phase portraits, Poincaré maps, and frequency spectra, illustrates these phenomena in greater detail, as depicted in [26].

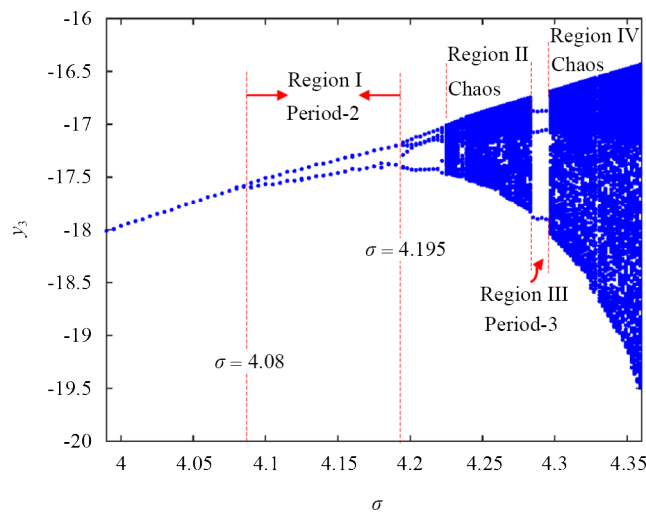


**Figure 1.** Motor angular speed bifurcation diagram with respect to  $\sigma$

The largest Lyapunov exponent provides a critical measure for identifying chaos within a dynamic system. By analyzing the spectrum of Lyapunov exponents ( $\lambda$ ) [12], changes in the system's length, area and volume in phase space can be evaluated. To determine the presence of chaos, it suffices to compute only the largest exponent, which reveals whether nearby trajectories diverge ( $\lambda > 0$ ) or converge ( $\lambda < 0$ ). Systems exhibiting bounded motion with at least one positive Lyapunov exponent are classified as chaotic, whereas periodic motions are characterized by non-positive exponents. Figure 2 presents the evolutions of the largest Lyapunov exponent in BLDCM systems, computed using the algorithm proposed by Wolf et al. [12]. The onset of chaotic motion corresponds to points  $P_3, P_4,$  and  $P_5$ , where the largest Lyapunov exponent transitions from negative to positive as parameter  $\sigma$  increases. At points  $P_1$  and  $P_2$ , the largest Lyapunov exponent approaches zero where the system is prone to bifurcation.

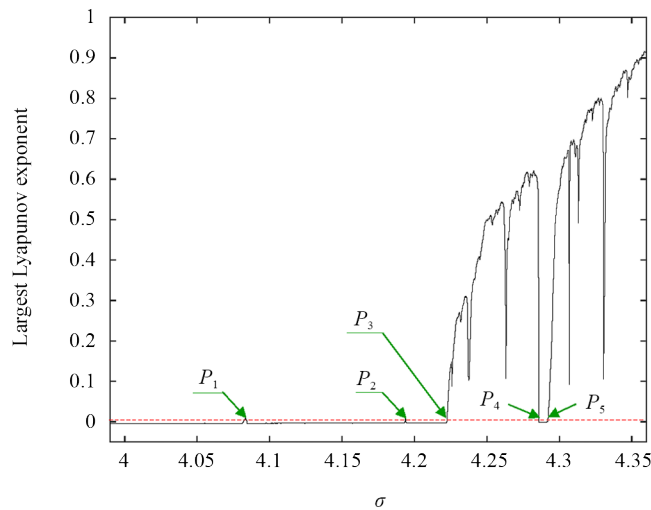


**Figure 2.** Evolutions of largest Lyapunov exponent across parameter changes

When parameter  $\sigma$  falls below  $P_2$ , the Lyapunov exponents calculated from Equations (4)-(6) become negative. For instance, at  $\sigma = 4.1$ , the values of the exponents are  $\lambda_1 = -0.0035045$ ,  $\lambda_2 = -0.2269056$  and  $\lambda_3 = -8.3870359$ . Negative values for all Lyapunov exponents indicate that the BLDCM is in a stable periodic state. Using the Lyapunov exponents  $\lambda_1 \geq \dots \geq \lambda_n$  of a dynamical system, Kaplan and Yorke [27] proposed a method to estimate the Lyapunov dimension  $d_L$  expressed as:

$$d_L = j + \frac{1}{|\lambda_{j+1}|} \sum_{i=1}^j \lambda_i, \quad \text{where } \sum_{i=1}^j \lambda_i > 0 \text{ and } \sum_{i=1}^{j+1} \lambda_i < 0 \quad (7)$$

Thus, the Lyapunov dimension is an integer for periodic orbit, but becomes a non-integer for chaotic behavior. Using Equations (4)-(6) with  $\sigma = 4.1$ , the Lyapunov dimension is calculated as  $d_L = 1$ , confirming that the system exhibits periodic motion because the Lyapunov dimension is an integer. When  $\sigma$  increases surpasses point  $P_3$ , such as at  $\sigma = 4.25$ , the Lyapunov exponents change to  $\lambda_1 = 0.4994983$ ,  $\lambda_2 = -0.0029595$ , and  $\lambda_3 = -9.3307454$ , yielding a Lyapunov dimension of  $d_L = 2.0535$ . This result indicates that the BLDCM system transitions to chaotic motion, as evidenced by the positive largest Lyapunov exponent and non-integer Lyapunov dimension.

### 3. Suppressing chaos by dither control

Understanding the behaviors of a chaotic system is beneficial; however, the ultimate goal is to achieve effective control over them. To enhance the performance of dynamic systems, it is necessary to convert chaotic motion into stable periodic motion. This section explains how chaotic motion can be controlled by introducing an external input, known as a dither signal, to adjust only the nonlinear components of the system. Due to its high frequency and periodic nature, a dither signal averages out nonlinearities. Recently, several dither smoothing techniques have been proposed [16, 17] to stabilize chaotic systems. Two common types of dither signals are described below [28].

#### 3.1 Square-wave dither

A square-wave dither signal is one of the simplest approaches, characterized by its frequency and amplitude, set at 2,000 rad/s and  $W$ , respectively. This signal modifies the effective value of the system's non-linearity  $f(\cdot)$  as follows:

$$\bar{n} = \frac{1}{2}[f(y+W) + f(y-W)] \quad (8)$$

As a result, the system equation can be expressed as:

$$\dot{y} = \bar{n} \quad (9)$$

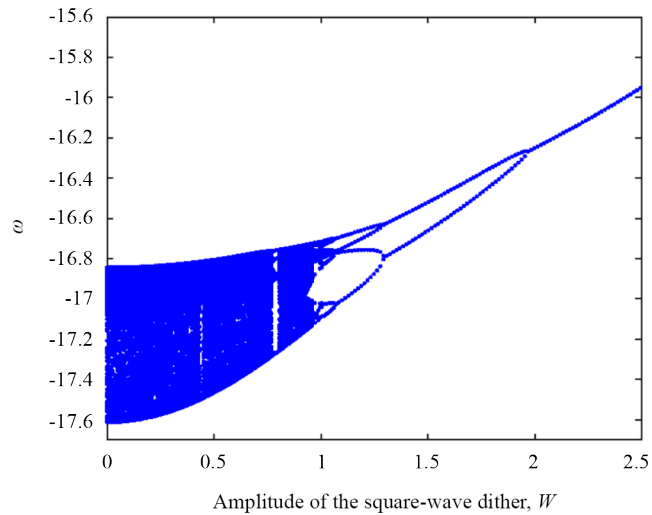


**Figure 3.** Bifurcation diagram illustrating the system's response to a square-wave dither, where  $W$  represents the amplitude of the applied signal

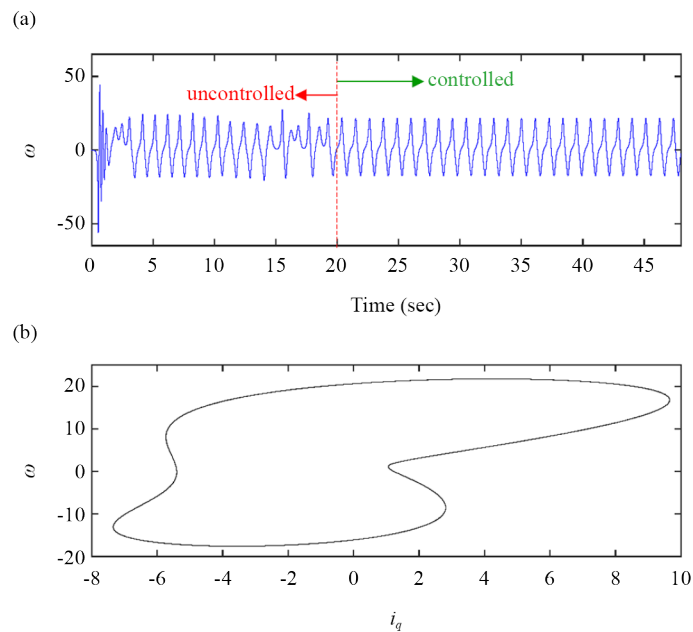


**Figure 4.** A square-wave dither signal applied to mitigate chaotic motion of the BLDCM system at  $\sigma = 4.26$  and  $W = 2.25$ : (a) system time responses; control signal activated after 20 s, (b) resulting controlled orbit phase portrait

To evaluate the impact of the square-wave dither, simulations were conducted with parameter  $\sigma = 4.26$ . By gradually increasing the dither amplitude from  $W = 0$  to 2.5, the chaotic motion transitions to period-one motion. Figure 3 shows the bifurcation diagram. Now, we select the amplitude of square-wave dither  $W = 2.25$ . Figure 4a plots the time response, where the square-wave dither signal is activated after 20 s. The chaotic behavior system is converted into a stable period-one orbit. Figure 4b illustrates the phase portrait of the controlled orbit.

### 3.2 Sinusoidal dither

A sinusoidal dither signal, another widely used technique, introduces a high-frequency oscillation. The effective value of  $n$  is calculated over a full oscillation cycle, given by:

$$n = \frac{1}{2\pi} \int_0^{2\pi} f(y + W \sin \theta) d\theta \quad (10)$$

Now, adding a sinusoidal dither signal to Equations (4)-(6) yields the following coupled system as follows:

$$\frac{d\tilde{y}_1}{dt} = \tilde{u}_q - \tilde{y}_1 + \rho\tilde{y}_3 - n_1 \quad (11)$$

$$\frac{d\tilde{y}_2}{dt} = \tilde{u}_d - \delta\tilde{y}_2 + n_2 \quad (12)$$

$$\frac{d\tilde{y}_3}{dt} = \sigma(\tilde{y}_1 - \tilde{y}_3) - \tilde{T}_L + \eta n_3 \quad (13)$$

where

$$n_1 = \frac{1}{2\pi} \int_0^{2\pi} (\tilde{y}_2 + W \sin \theta)(\tilde{y}_3 + W \sin \theta) d\theta$$

$$n_2 = \frac{1}{2\pi} \int_0^{2\pi} (\tilde{y}_1 + W \sin \theta)(\tilde{y}_3 + W \sin \theta) d\theta$$

$$n_3 = \frac{1}{2\pi} \int_0^{2\pi} (\tilde{y}_1 + W \sin \theta)(\tilde{y}_2 + W \sin \theta) d\theta$$

The frequency of the sinusoidal dither must significantly exceed all other frequencies present in the system's operation. Failing to meet this condition could result in the dither signal inducing an unwanted oscillation at its own frequency. For the current system, let  $\sigma = 4.26$  and set the sinusoidal dither frequency to 4,000 rad/s. The bifurcation diagram in Figure 5 illustrated that when the dither amplitude exceeds 1.15 V, the chaotic behavior of the BLDCM system transitions into a stable periodic motion. Specifically, with a sinusoidal dither amplitude of  $W = 1.3$  and frequency = 4,000 rad/s, applied after 6 s, the system initially exhibits chaotic behavior but subsequently stabilizes into periodic motion, as demonstrated in Figure 6.

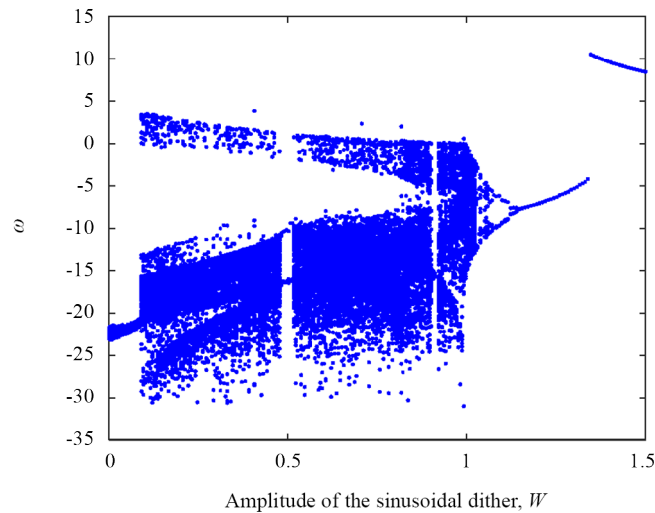


**Figure 5.** Bifurcation diagram showcases the effects of sinusoidal dither, with  $W$  indicating the amplitude of the sinusoidal signal

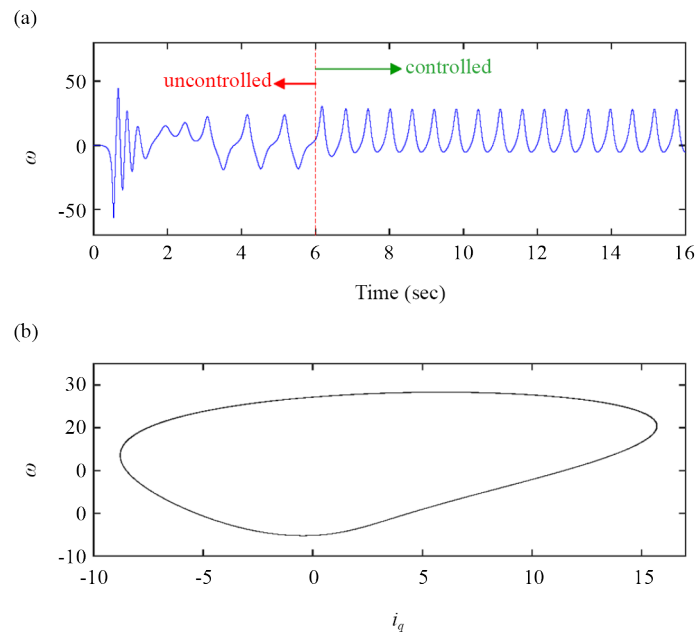


**Figure 6.** Transition from chaotic motion to period-one orbit for  $W = 1.3$  and  $\sigma = 4.26$ : (a) time response showing control signal application after 6 s, (b) phase portrait of the stabilized system

## 4. Conclusions

This study examined the complex nonlinear dynamics of a BLDCM system and the challenges associated with controlling chaos. By utilizing bifurcation diagrams, the dynamic behavior across a wide range of parameter values was analyzed. The transitions to chaotic motion were identified as period-doubling and period-3 bifurcation. To determine whether the system exhibits chaotic motion, the Lyapunov exponents and Lyapunov dimensions proved to be reliable diagnostics tools for assessing chaos in BLDCM systems. Finally, square-wave and sinusoidal dither signals were demonstrated to effectively convert chaotic motion into periodic motion by being applied before the nonlinearity in the chaotic system. For sinusoidal dither signals, maintaining a high frequency is essential to ensure their effectiveness.

Other numerous methods for chaos control, such as synchronization control, time-delayed feedback control, neuro-fuzzy control, adaptive control and bang-bang control, have also been developed. However, this study highlights that dither signal control offers a simple and practical solution for suppressing chaos in BLDCM systems. The effectiveness of these proposed chaos control strategies was validated through numerical simulations, showing that they are not only efficient but also easy to implement compared to alternative methods.

An enhanced understanding of the dynamics and chaos control in BLDCM systems has the potential to contribute to the advancements in electric vehicle technologies. The considered BLDCM system can be adapted to model real-world applications in future research. Figure 7 provides a schematic representation of the experimental setup. The dither signal was generated using a function generator with a frequency range of 0-10,000 Hz, while waveform analysis was conducted with an HP 3562A dynamic signal analyzer. Analog signal was amplified using a voltage amplifier and a servo amplifier to drive the DC motor.

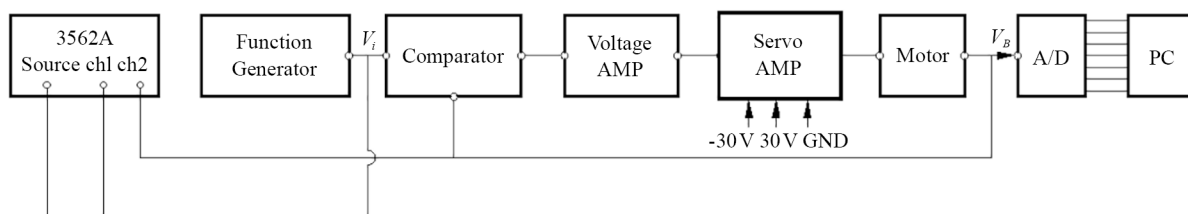


Figure 7. Schematic representation of the experimental set-up

## Acknowledgements

This research was supported by the Ministry of Science and Technology of Taiwan (R.O.C.) under grant number MOST 108-2221-E-212-010-MY3.

## Conflict of interest

The author confirms that there is no conflict of interest.

## References

- [1] Naseri F, Farjah E, Ghanbari T. An efficient regenerative braking system based on battery/supercapacitor for electric, hybrid, and plug-in hybrid electric vehicles with BLDC motor. *IEEE Transactions on Vehicular Technology*. 2016; 66(5): 3724-3738. Available from: <https://doi.org/10.1109/TVT.2016.2611655>.
- [2] Zhang G, Deng J, Fu N. Minimum copper loss direct torque control of brushless DC motor drive in electric and hybrid electric vehicles. *IEEE Access*. 2019; 7: 113264-113271. Available from: <https://doi.org/10.1109/ACCESS.2019.2927416>.
- [3] Liu Y, Zhou Y, Cao J. Design of small BLDCM for aircraft fuel pump. In: *Asia-Pacific International Symposium on Aerospace Technology*. Singapore: Springer; 2018. p.2719-2725. Available from: [https://doi.org/10.1007/978-981-13-3305-7\\_219](https://doi.org/10.1007/978-981-13-3305-7_219).
- [4] Liu K, Fu X, Lin M, Tai L. AC copper losses analysis of the ironless brushless DC motor used in a flywheel energy storage system. *IEEE Transactions on Applied Superconductivity*. 2016; 26(7): 1-5. Available from: <https://doi.org/10.1109/TASC.2016.2602500>.
- [5] Yang W, Ma R, Li T, Mi Q, Zhang Z, Peng J. Speed synchronous control of dual-BLDCMs based on MRAC for a hoist application. In: *IECON 2021-47th Annual Conference of the IEEE Industrial Electronics Society*. Toronto, ON, Canada: IEEE; 2021. p.1-6. Available from: <https://doi.org/10.1109/IECON48115.2021.9589969>.



- [6] Chen S, Liu G, Zheng S. Sensorless control of BLDCM drive for a high-speed maglev blower using low-pass filter. *IEEE Transactions on Power Electronics*. 2016; 32(11): 8845-8856. Available from: <https://doi.org/10.1109/TPEL.2016.2645782>.
- [7] Sarwardi S, Hossain S, Sajid M, Almohaimed AS. Analysis of the Bogdanov-Takens bifurcation in a retarded oscillator with negative damping and double delay. *AIMS Mathematics*. 2022; 7(11): 19770-19793. Available from: <https://doi.org/10.3934/math.20221084>.
- [8] Sajid M. Chaotic behaviour and bifurcation in real dynamics of two-parameter family of functions including logarithmic map. *Abstract and Applied Analysis*. 2020; 2020(1): 7917184. Available from: <https://doi.org/10.1155/2020/7917184>.
- [9] Gökçen A, Soydemir MU, Şahin S. Chaos control of BLDC motor via fuzzy based PID controller. In: *Intelligent and Fuzzy Techniques: Smart and Innovative Solutions: Proceedings of the INFUS 2020 Conference*. Istanbul, Turkey; p.1540-1547. Available from: [https://doi.org/10.1007/978-3-030-51156-2\\_179](https://doi.org/10.1007/978-3-030-51156-2_179).
- [10] Faradja P, Qi G. Local bifurcation analysis of brushless DC motor. *International Transactions on Electrical Energy Systems*. 2019; 29(2): e2710. Available from: <https://doi.org/10.1002/etep.2710>.
- [11] Zhong X, Shahidehpour M, Zou Y. Global quasi-Mittag-Leffler stability of distributed-order BLDCM system. *Nonlinear Dynamics*. 2022; 108(3): 2405-2416. Available from: <https://doi.org/10.1007/s11071-022-07304-x>.
- [12] Wolf A, Swift JB, Swinney HL, Vastano JA. Determining Lyapunov exponent from a time series. *Physica D: Nonlinear Phenomena*. 1985; 16(3): 285-317. Available from: [https://doi.org/10.1016/0167-2789\(85\)90011-9](https://doi.org/10.1016/0167-2789(85)90011-9).
- [13] Li ZB, Lu W, Gao LF, Zhang JS. Nonlinear state feedback control of chaos system of brushless DC motor. *Procedia Computer Science*. 2021; 183: 636-640. Available from: <https://doi.org/10.1016/j.procs.2021.02.108>.
- [14] Wang C, Zhang H, Fan W, Ma P. Adaptive control method for chaotic power systems based on finite-time stability theory and passivity-based control approach. *Chaos, Solitons & Fractals*. 2018; 112: 159-167. Available from: <https://doi.org/10.1016/j.chaos.2018.05.005>.
- [15] Moustafa E, Sobaih AA, Abozalam B, Mahmoud ASA. Period-doubling bifurcation analysis and chaos control for load torque using FLC. *Complex & Intelligent Systems*. 2021; 7: 1381-1389. Available from: <https://doi.org/10.1007/s40747-021-00276-2>.
- [16] Fuh CC, Tung PC. Experimental and analytical study of dither signals in a class of chaotic system. *Physics Letters A*. 1997; 229(4): 228-234. Available from: [https://doi.org/10.1016/S0375-9601\(97\)00153-9](https://doi.org/10.1016/S0375-9601(97)00153-9).
- [17] Liaw YM, Tung PC. Application of the differential geometric method to control a noisy chaotic system via dither smoothing. *Physics Letters A*. 1998; 239(1-2): 51-58. Available from: [https://doi.org/10.1016/S0375-9601\(97\)00919-5](https://doi.org/10.1016/S0375-9601(97)00919-5).
- [18] Tung PC, Chen SC. Experimental and analytical studies of the sinusoidal dither signal in a DC motor system. *Dynamics and Control*. 1993; 3(1): 53-69. Available from: <https://doi.org/10.1007/BF01968359>.
- [19] Chang SC, Lin BC, Lue YF. Dither signal effects on quenching chaos of a permanent magnet synchronous motor in electric vehicles. *Journal of Vibration and Control*. 2011; 17(12): 1912-1918. Available from: <http://dx.doi.org/10.1177/1077546310395978>.
- [20] Hemati N, Leu MC. A complete model characterization of brushless DC motors. *IEEE Transactions on Industry Applications*. 1992; 28(1): 172-180. Available from: <https://doi.org/10.1109/28.120227>.
- [21] Hemati N. Strange attractors in brushless DC motors. *IEEE Transactions on Circuits and Systems I: Fundamental Theory and Applications*. 1994; 41(1): 40-45. Available from: <https://doi.org/10.1109/81.260218>.
- [22] Hemati N. Dynamic analysis of brushless motors based on compact representations of the equations of motion. In: *Conference Record of the 1993 IEEE Industry Applications Conference Twenty-Eighth IAS Annual Meeting*. Toronto, ON, Canada: IEEE; 1993. p.51-58. Available from: <https://doi.org/10.1109/IAS.1993.298903>.
- [23] Roy P, Ray S, Bhattacharya S. Control of chaos in brushless DC motor design of adaptive controller following backstepping method. In: *Proceedings of the 2014 International Conference on Control, Instrumentation, Energy and Communication (CIEC)*. Calcutta, India: IEEE; 2014. p.41-45. <https://doi.org/10.1109/CIEC.2014.6959046>.
- [24] Ge ZM, Chang CM, Chen YS. Anti-control of chaos of single time scale brushless dc motors and chaos synchronization of different order systems. *Chaos, Solitons & Fractals*. 2006; 27: 1298-1315. Available from: <https://doi.org/10.1016/j.chaos.2005.04.095>.
- [25] *User's Manual-IMSL MATH/LIBRARY*. Houston, TX, USA: IMSL, Inc.; 1989.
- [26] Chang SC. Analytical routes to chaos and controlling chaos in brushless DC motors. *Processes*. 2022; 10(5): 814. Available from: <https://doi.org/10.3390/pr10050814>.

- [27] Kaplan JL, Yorke JA. Chaotic behavior of multidimensional difference equations. In: *Functional Differential Equations and Approximation of Fixed Points: Proceedings*. Bonn, Germany; 1979. p.204-227. Available from: <https://doi.org/10.1007/BFb0064319>.
- [28] Cook PA. *Nonlinear Dynamical Systems*. London, UK: Prentice-Hall; 1994.